Heat Treatment and Thermal Characterization of Ni-Rich Niti Manufactured via Laser Powder Bed Fusion

*Lehar Asip Khan[1,2,4],Sumaiya Malik[3], Muhammad Mubashar Saeed[4], Hasan Ayub[1,2,4], Ahmar Murtaza[4], Inam Ul Ahad[1,2,4] and Dermot Brabazon[1,2,4]

[1]I-Form Advanced Manufacturing Research Centre, School of Mechanical and Manufacturing Engineering, Dublin City University, Dublin, Ireland
[2]Advanced Processing Technology Research Centre, School of Mechanical & Manufacturing Engineering, Dublin City University, Dublin, Ireland
[3]Department of Mathematics, University of Sargodha, Sargodha, Pakistan
[4]Dublin City University, School of Mechanical and Manufacturing Engineering
lehar.khan3@mail.dcu.ie

Abstract. Nitinol (NiTi) alloy consists of nickel (Ni) and titanium (Ti) shows the shape retention and psuedoelasticity while going through phase transformation. NiTi is a strong candidate for engineering applications due to these properties. In this work, NiTi tubes were manufactured via LPBF starting from NiTi powder with (52%Ni-48%Ti). Heat treatment was performed at a continuous temperature of 500 ºC for 10 min to 60 min. Heat flow analysis shows an increase in austenite finish temperature to 25 ºC. The experiments for thermal expansion coefficient (CTE) shows values of $11.4x10^{-6}$/°C that matached with literature for austenitic thermal expansion coefficient.

Keywords: Nitinol, PBF-LB, , Phase transformation

1 Introduction

Nitinol (NiTi) alloy exists in the binary composition of nickel (Ni) and titanium (Ti) ranging from 45% (at.%) to 55% (at. %) for both Ni and Ti respectively [1], [2]. Primarily, NiTi has two solid phases martensite (lowtemperature phase) and austenite (high-temperature phase). Martensite has a monoclinic crystal structure while austenite has a cubic center crystal structure. NiTi exhibits shape memory and superelastic properties depending upon the exact composition i.e. Ni: Ti [3]–[5], which makes it an interesting material for potential engineering applications in various industries such as biomedical engineering, aerospace, and automotive industries [6]–[9]. Ni-rich NiTi results in an austenite phase at room temperature exhibiting superelasticity while Ti-rich results in a martensite phase at room temperature showing shape memory property. NiTi is manufactured widely via the casting technique while metal additive manufacturing (metal AM) is an emerging technology that is also used [10], [11]. On a very large scale, NiTi wires and tubes are manufactured using casting technology employed in various applications. However, in the last few decades, metal AM has also been used in manufacturing NiTi providing similar thermal/physical properties to the manufactured parts. Moreover, metal AM has numerous advantages over the casting

I. U. Ahad (ed.), *Proceedings of the 4th International Conference on Key Enabling Technologies (KEYTECH 2024)*, Atlantis Highlights in Engineering 35,
https://doi.org/10.2991/978-94-6463-602-4_36

technology such as, near net-shaped parts, freedom to manufacture complex geometries, and less waste etc [12]–[19]. NiTi goes through solid-solid phase transformation from martensiteaustenite and austenite to martensite with transformation temperature majorly dependent upon composition. However, the transformation temperature is altered using the ageing heat treatment of NiTi. Numerous studies have been reported in the literature on studying the change in austenite finish temperatures after performing ageing heat treatment on NiTi [20]–[24].

In this study, NiTi tubes produced by metal additive manufacturing (AM) underwent aging heat treatment in a furnace under an inert atmosphere. The tubes were subjected to consistent heating at a fixed temperature for specific durations to investigate the impact of heat treatment. Various thermal and physical characterization methods were applied to assess the effects of the treatment, including relative density measurements, thermal heat flow analysis, and evaluations of the thermal expansion coefficient (CTE).

2.Materials and Methodologies

NiTi tubes produced through casting were supplied by Johnson Matthey (JM) PLC, with atomic percentages of 50.8% Nickel and 49.2% Titanium. JM utilized the casting process, which involved melting and drawing, to manufacture these tubes, and their austenite finish temperature, measured through a three-point bending test, was 1.7°C. Additionally, NiTi tubes were fabricated using the metal additive manufacturing (AM) method of Laser Powder Bed Fusion (PBF-LB), starting with NiTi powder containing 52% Nickel and 48% Titanium. The composition of the pre-alloyed NiTi powder used in this process was confirmed through Energy Dispersive X-ray (EDX) analysis. Furthermore, the particle size distribution and powder morphology are illustrated in **Fig. 1** (a) and (b).

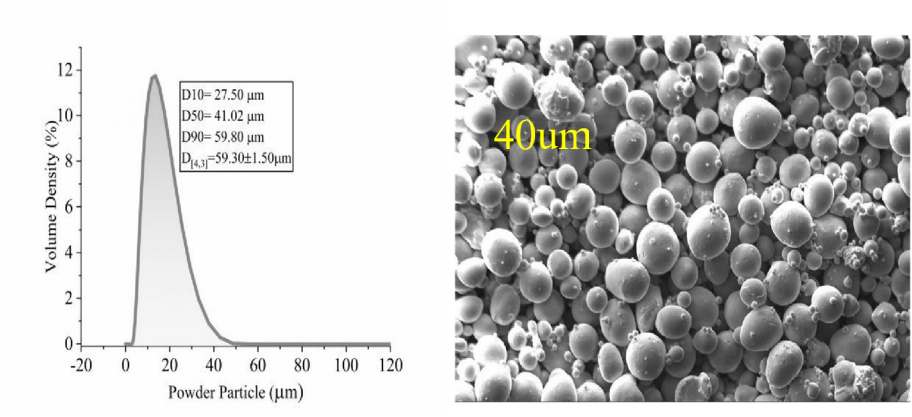

(a) (b)

Fig. 1. Powder morphology analysis: (a) The size distribution of the sieved powder material prior to the additive manufacturing process, and (b) Scanning electron microscopy (SEM) images of the powder before undergoing additive manufacturing.

The relative density of the as-received (JM), as-manufactured (PBF-LB), and heat-treated samples was measured using the Archimedes method in accordance with ASTM B962-17 standards. These measurements, performed in both ethanol and air, utilized the Sartorius Entris II Essential BCE124I-1S device, offering a repeatability and accuracy of ±0.0001g. A reference density of 6450 kg/m³ was applied for NiTi in the calculations [25]. Heat flow analysis was conducted through differential scanning calorimetry (DSC) to assess the phase transformation temperatures before and after heat treatment, using a TA Instruments DSC 2500, following ASTM F2004 standards. The samples were heated and cooled at a rate of 10°C/min. The thermal expansion coefficients (CTEs) were measured via dilatometry, using a Netzsch DIL 402PC, on both untreated and heat-treated NiTi tubes. Calibration and sample preparation followed ASTM E228-17 guidelines [26]. The tubes were heated slowly under a continuous Argon gas flow to prevent oxidation. Furnace heat treatment was carried out at a constant temperature of 500°C, ensuring a steady Argon flow to avoid oxidation. **Table 1** outlines the durations of heat treatment at this fixed temperature.

Table 1. The heat treatment parameters for metal AM NiTi tube

AM samples heat treated	Time (min)
Metal AM as Printed	-
Sample 1 (S1)	10 min
Sample 2 (S2)	30 min
Sample 3 (S3)	60 min

2.1 Results and Discussion

DSC for PBF-LB NiTi tubes

The differential scanning calorimetry (DSC) curves and phase transformation temperatures for metal AM samples, both in their as-printed and heat-treated states, are presented in Figure 2. Table 2 summarizes the thermal and phase transformation properties of these samples. After heat treatment, the samples were quenched in water at room temperature. Heating the material at 500°C for 10 minutes successfully eliminated the unstable R* phase, thereby stabilizing the phase transformation and increasing the transition enthalpy by 69% to 9.52 J/g, as depicted in Fig. 2(b). This stabilization expanded the transformation range, resulting in an austenite start temperature (As) of 10.05°C and an austenite finish temperature (Af) of 22.54°C. With a 30-minute heat treatment, the transition enthalpy rose to 17.48 J/g, and the Af increased to 23.86°C, marking a 45% improvement over sample S1 (enthalpy = 9.52 J/g). A 60-minute heat treatment achieved an Af of 25.4°C and a transformation enthalpy of 17.14 J/g, closely matching sample S3. During the cooling phase of the heat-treated samples, the martensitic R* phase reappeared in the NiTi tubes, corroborating the findings of Khan et al. [4], [27].

Table 2. Summary of thermal and physical properties for as-printed and heat-treated NiTi samples produced via Laser Powder Bed Fusion

Samples	A_s (ºC)	A_f (ºC)	ΔH_A (J/g)	$\lvert\Delta T_A\rvert$ (ºC)	M_s (ºC)	M_f (ºC)	ΔH_M (J/g)	$\lvert\Delta T_M\rvert$ (ºC)
As-printed	9.67	31.24	2.89	21.57	30.89	2.16	3.67	28.73
S1	10.05	22.54	9.52	12.49	-21.24	-46.68	3.59	25.44
S2	11.93	23.86	17.48	11.93	-20.44	-43.13	7.25	22.69
S3	14.7	25.4	17.14	10.7	-13.51	-35.8	8.33	22.29

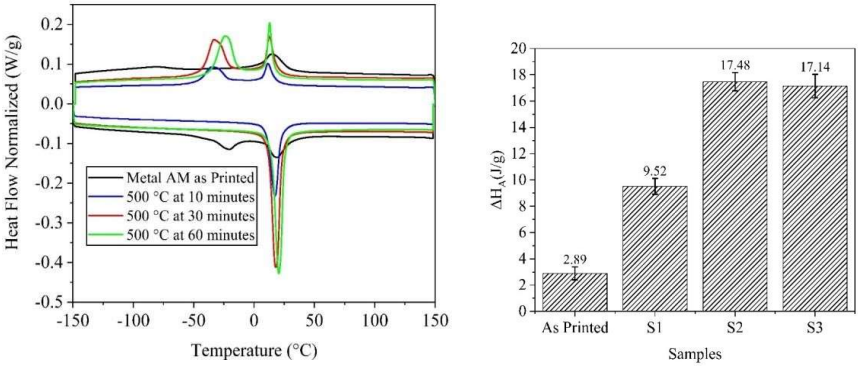

(a) (b)

Fig. 2. The differential scanning calorimetry (DSC) curves and phase transformation temperatures for metal AM samples, both in their as-printed and heat-treated states, are shown.

2.2 Thermal expansion coefficients

Fig. 3 (a) illustrates the changes in the thermal expansion coefficient (CTE) of the metal AM tube as a function of temperature without post-processing. Initially, the tube is in the martensitic phase, with a CTE of $8x10^{-6}$/°C up to 60°C, which then increases to $10x10^{-6}$/°C by 110°C. Beyond this point, there is a sharp decrease, stabilizing at a CTE of approximately $11.4x10^{-6}$/°C, indicating the onset of the austenitic phase [28]. The irregular expansion is likely due to residual stresses introduced during the PBF-LB manufacturing process [29]. To address these stresses, various post-processing methods are typically applied after additive manufacturing. **Fig. 3** (b) shows the thermal expansion behavior of the tube after 30 minutes of heat treatment. Notably, there are no traces of the CTE values characteristic of the martensitic phase ($8x10^{-6}$/°C), with a consistent average CTE of around $11.4x10^{-6}$/°C. **Fig. 3** (c) presents the CTE results for

the tube heat-treated for 60 minutes, which also exhibits a stable CTE evolution, confirming the presence of the austenitic phase.

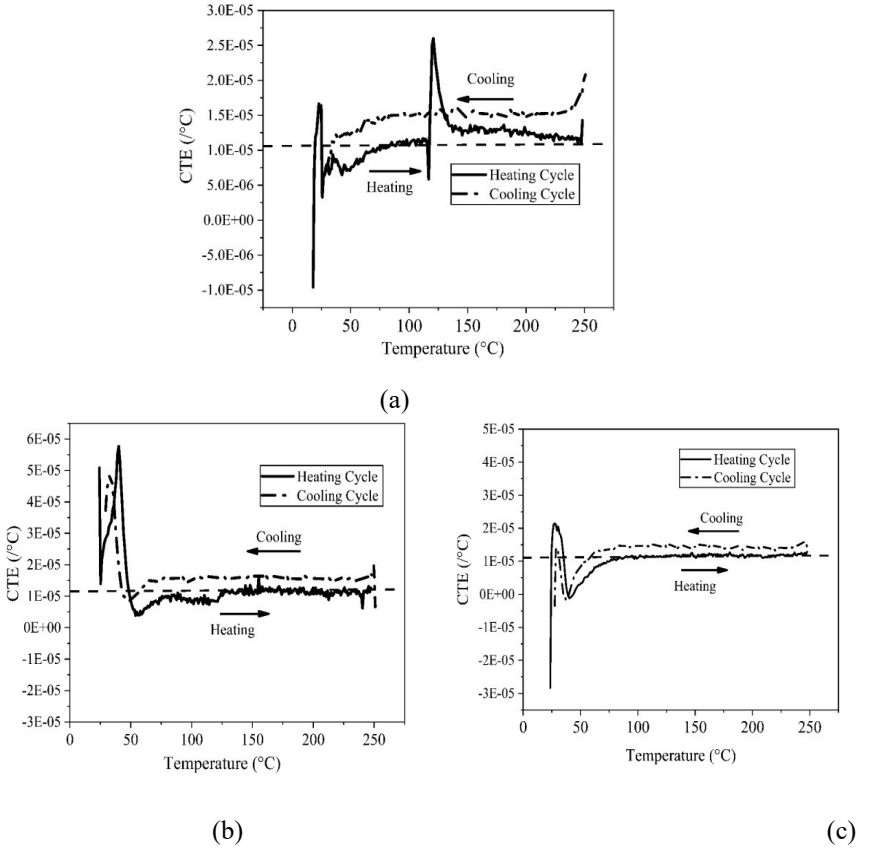

Fig. 3. Thermal expansion coefficients for metal AM tubes **(a)** as printed, **(b)** heat treated for 30 min at a temperature of 500 °C **(c)** heat treated for 60 min at a temperature of 500 °C.

3 Conclusion

This study investigated the impact of furnace heat treatment on NiTi tubes produced through metal additive manufacturing (PBF-LB). Thermal analysis was conducted on both the as-manufactured and heat-treated NiTi samples using differential scanning calorimetry (DSC) and dilatometry. The heat flow analysis, which measured phase transformation temperatures, showed an increase in the austenite finish temperature of the NiTi tubes following heat treatment, reaching 25.4°C. Additionally, a thermal expansion coefficient of 11.4×10^{-6}/°C was observed, aligning well with results reported in the literature.

Acknowledgement. This work is supported in part by a research grant from Enterprise Ireland and the Department of Business, Enterprise, and Innovation under Grant Number DT 201 9 0076.

References

[1] J. Mohd Jani, M. Leary, A. Subic, and M. A. Gibson, "A review of shape memory alloy research, applications and opportunities," *Mater. Des.*, vol. 56, pp. 1078–1113, 2014, doi: 10.1016/j.matdes.2013.11.084.

[2] M. Elahinia, N. Shayesteh Moghaddam, M. Taheri Andani, A. Amerinatanzi, B. A. Bimber, and R. F. Hamilton, "Fabrication of NiTi through additive manufacturing: A review," *Prog. Mater. Sci.*, vol. 83, pp. 630–663, 2016, doi: 10.1016/j.pmatsci.2016.08.001.

[3] L. A. Khan, H. Ayub, J. C. Chekotu, K. Tamilselvam, C. Muilwijk, I. U. Ahad, and D. Brabazon, "Steady-state and transient mechanical response analysis of superelastic nitinol lattice structures prior to additive manufacturing: an insilico study," *J. Mater. Res. Technol.*, 2023, doi: 10.1016/j.jmrt.2023.06.137.

[4] L. A. Khan, E. Mccarthy, I. U. Ahad, and D. Brabazon, "Analysis of nitinol actuator response under controlled conductive heating regimes," *Results Eng.*, vol. 18, no. January, 2023, doi: 10.1016/j.rineng.2023.101047.

[5] L. A. Khan, C. Muilwijk, H. Ayub, I. U. Ahad, and D. Brabazon, "Effect of post-heat-treatment on thermal and
physical characteristics of NiTi tubes produced via conventional drawing and laser powder bed fusion," *J. Mater. Res. Technol.*, vol. 26, pp. 6609–6622, 2023, doi: https://doi.org/10.1016/j.jmrt.2023.09.012.

[6] S. L. Menu, *Recent Advances in Mechanical*, vol. 17, no. 3. 2004.

[7] A. Behera, A. K. Sahoo, and S. S. Mohapatra, "14 - Nickel–titanium smart hybrid materials for automotive industry," in *Micro and Nano Technologies*, S. Thomas, A. Behera, and T. A. B. T.-N.-T. S. H. M. Nguyen, Eds., Elsevier, 2022, pp. 271–295. doi: https://doi.org/10.1016/B978-0-323-91173-3.00015-8.

[8] J. Ko, S. Bhullar, Y. Cho, P. C. Lee, and M. Byung-Guk Jun, "Design and fabrication of auxetic stretchable force sensor for hand rehabilitation," *Smart Mater. Struct.*, vol. 24, no. 7, 2015, doi: 10.1088/0964-1726/24/7/075027.

[9] D. J. Hartl and D. C. Lagoudas, "Aerospace applications of shape memory alloys," *Proc. Inst. Mech. Eng. Part G J.*

Aerosp. Eng., vol. 221, no. 4, pp. 535–552, 2007, doi: 10.1243/09544100JAERO211.

[10] Johnson Matthey, "Nitinol technical properties." https://matthey.com/en/products-and-services/medicalcomponents/resource-library/nitinol-technical-properties

[11] Fort Wayne Metals, "Nitinol – Fort Wayne Metals," 2020. https://fwmetals.de/materials/nitinol/ (accessed Mar. 01, 2023).

[12] M. A. Obeidi, “Additive Design Mimics the Strength and Architect of Nature,” pp. 1–11, 2023.

[13] A. Mussatto, R. Groarke, A. O’Neill, M. A. Obeidi, Y. Delaure, and D. Brabazon, “Influences of powder morphology and spreading parameters on the powder bed topography uniformity in powder bed fusion metal additive manufacturing,” *Addit. Manuf.*, vol. 38, no. December 2020, p. 101807, 2021, doi: 10.1016/j.addma.2020.101807.

[14] R. McCann, M. A. Obeidi, C. Hughes, É. McCarthy, D. S. Egan, R. K. Vijayaraghavan, A. M. Joshi, V. Acinas Garzon, D. P. Dowling, P. J. McNally, and D. Brabazon, “In-situ sensing, process monitoring and machine control in Laser Powder Bed Fusion: A review,” *Addit. Manuf.*, vol. 45, no. May, 2021, doi: 10.1016/j.addma.2021.102058.

[15] M. A. Obeidi, M. Monu, C. Hughes, D. Bourke, M. N. Dogu, J. Francis, M. Zhang, I. U. Ahad, and D. Brabazon,
“Laser beam powder bed fusion of nitinol shape memory alloy (SMA),” *J. Mater. Res. Technol.*, vol. 14, pp. 2554– 2570, 2021, doi: 10.1016/j.jmrt.2021.07.126.

[16] M. N. DOGU, S. Ozer, M. A. Yalçın, K. Davut, G. M. Bilgin, M. A. Obeidi, H. Brodin, H. Gu, and D. Brabazon,
“Effect of Solution Heat Treatment on the Microstructure and Crystallographic Texture of In939 Fabricated by Powder Bed Fusion-Laser Beam,” *SSRN Electron. J.*, 2023, doi: 10.2139/ssrn.4365807.

[17] M. A. Obeidi, A. Conway, A. Mussatto, M. N. Dogu, S. P. Sreenilayam, H. Ayub, I. U. Ahad, and D. Brabazon, “Effects of powder compression and laser re-melting on the microstructure and mechanical properties of additively manufactured parts in laser-powder bed fusion,” *Results Mater.*, vol. 13, no. February, p. 100264, 2022, doi: 10.1016/j.rinma.2022.100264.

[18] M. A. Obeidi, I. U. Ahad, and D. Brabazon, “Investigating the Melt-Pool Temperature Evolution in Laser-Powder Bed Fusion by Means of Infra-Red Light: A Review,” *Key Eng. Mater.*, vol. 926 KEM, pp. 235–241, 2022, doi: 10.4028/p-6fn67z.

[19] A. Mussatto, R. Groarke, A. O’Neill, M. A. Obeidi, Y. Delaure, and D. Brabazon, “Influences of powder morphology and spreading parameters on the powder bed topography uniformity in powder bed fusion metal additive manufacturing,” *Addit. Manuf.*, vol. 38, no. December 2020, p. 101807, 2021, doi: 10.1016/j.addma.2020.101807.

[20] J. Zhu, Q. Zeng, and T. Fu, “An updated review on TiNi alloy for biomedical applications,” vol. 37, no. 6, pp. 539– 552, 2019, doi: doi:10.1515/corrrev-2018-0104.

[21] N. Sabahi, W. Chen, C. H. Wang, J. J. Kruzic, and X. Li, “A Review on Additive Manufacturing of Shape-Memory Materials for Biomedical Applications,” *Jom*, vol. 72, no. 3, pp. 1229–1253, 2020, doi: 10.1007/s11837-020-04013x.

[22] E. Farber, J.-N. Zhu, A. Popovich, and V. Popovich, “A review of NiTi shape memory alloy as a smart material produced by additive manufacturing,” *Mater. Today Proc.*, vol. 30, pp. 761–767, 2020.

[23] X. Wang, S. Kustov, and J. Van Humbeeck, "A short review on the microstructure, transformation behavior and functional properties of NiTi shape memory alloys fabricated by selective laser melting," *Materials (Basel).*, vol. 11, no. 9, p. 1683, 2018.

[24] C. Tan, S. Li, K. Essa, P. Jamshidi, K. Zhou, W. Ma, and M. M. Attallah, "Laser Powder Bed Fusion of Ti-rich TiNi
lattice structures: Process optimisation, geometrical integrity, and phase transformations," *Int. J. Mach. Tools Manuf.*, vol. 141, pp. 19–29, 2019, doi: https://doi.org/10.1016/j.ijmachtools.2019.04.002.

[25] Z. Yan, J.-N. Zhu, E. Borisov, T. Riemslag, S. P. Scott, M. Hermans, J. Jovanova, and V. Popovich, "Superelastic
Response and Damping Behaviour of Additively Manufactured Nitinol Architectured Materials," *Addit. Manuf.*, vol. 68, no. February, p. 103505, 2023, doi: 10.1016/j.addma.2023.103505.

[26] J. C. Chekotu, R. Goodall, D. Kinahan, and D. Brabazon, "Control of Ni-Ti phase structure, solid-state transformation temperatures and enthalpies via control of L-PBF process parameters," *Mater. Des.*, vol. 218, p. 110715, 2022, doi: 10.1016/j.matdes.2022.110715.

[27] L. A. Khan, H. Ayub, C. Muilwijk, E. McCarthy, I. U. Ahad, and D. Brabazon, "Experimental Analysis of R-Phase NiTi Tube Actuators Using in Contact Conductive Heating Stage BT - TMS 2023 152nd Annual Meeting & Exhibition Supplemental Proceedings," Cham: Springer Nature Switzerland, 2023, pp. 1293–1301.

[28] W. B. Cross, A. H. Kariotis, and F. J. Stimler, "Nitinol characterization study," NASA, 1969.

[29] M. C. C. Monu, E. J. Ekoi, C. Hughes, S. Sujith Kumar, and D. Brabazon, "Resultant physical properties of as-built nitinol processed at specific volumetric energy densities and correlation with in-situ melt pool temperatures," *J. Mater. Res. Technol.*, vol. 21, pp. 2757–2777, 2022, doi: 10.1016/j.jmrt.2022.10.073.